JOURNAL OF MECHANICAL ENGINEERING AND SCIENCES
ISSN: 2289-4659 e-ISSN: 2231-8380
VOLUME 20, ISSUE 1, 2026, 11126 - 11135
DOI: https://doi.org/10.15282/jmes.20.1.2026.8.0868

RESEARCH ARTICLE

Dual-layer smart coating system with a hybrid corrosion inhibitor for improved durability of carbon steel pipeline

K. Jayabalan[1], F.H.A. Rahim[1]*, P.S.M. Megat-Yusoff[1], N.F.C. Lah[1], R. Abdul Majid[2], S. Shaharuddin[3], S.H. Ramli[4]

[1]Department of Mechanical Engineering, Universiti Teknologi PETRONAS, Bandar Seri Iskandar, Perak, Malaysia
[2]Faculty of Chemical and Energy Engineering, Universiti Teknologi Malaysia (UTM), Johor, Malaysia
[3]Plant Engineering Technology, Universiti Kuala Lumpur (UniKL) MITEC, Kuala Lumpur, Malaysia
[4]Materials, Corrosion & Inspection (MCI), Group Technology Solution, PETRONAS, Malaysia

Abstract- This study aims to develop a hybrid dual-layer smart coating system incorporating multiple corrosion inhibitors to enhance the durability and corrosion resistance of carbon steel substrates. The proposed system consists of a hydrophobic zinc oxide–stearic acid (ZnO-STA) top layer and a self-healing epoxy bottom layer containing benzotriazole-loaded halloysite nanotubes (BTA-HNT) and boiled linseed oil microcapsules (BLO-MC). Five coating systems were fabricated, including pure epoxy, conventional dual-layer coating, and hybrid dual-layer coatings with ZnO-to-epoxy ratios of 2:1, 4:1, and 6:1. Structural and chemical characteristics were verified using Fourier Transform Infrared Spectroscopy (FTIR) and Scanning Electron Microscopy with Energy Dispersive X-ray Spectroscopy. At the same time, corrosion performance was evaluated using Electrochemical Impedance Spectroscopy and scratch tests over 2 weeks of immersion in 3.5 wt.% NaCl solution. The results indicate that the hybrid coating with a ZnO: epoxy ratio of 4:1 exhibited the best corrosion resistance, maintaining impedance values between 4.45 Ω and 4.16 Ω at low frequency and showing the lowest corrosion area of 4.4% after 2 weeks of exposure. However, the hybrid coatings demonstrated reduced adhesion strength, approximately 77.30% lower than the conventional dual-layer coating. Overall, the integration of ZnO-STA, BTA-HNT, and BLO-MC in a hybrid dual-layer system enhances corrosion protection through synergistic hydrophobic barrier and self-healing mechanisms. However, further optimisation is required to improve coating adhesion for long-term application.

Article History
Received : 30 July 2025
Revised : 23 February 2026
Accepted : 16 March 2026
Published : 31 March 2026

Keywords
Corrosion inhibitor
Electrochemical impedance
Hydrophobic
BTA-HNT

1. Introduction

Corrosion poses a major threat to oil and gas pipelines, resulting in costly maintenance and potentially decreasing the service life and structural integrity of these critical infrastructure systems. This problem encompasses the risk of sudden leak failure, which requires expensive repairs and replacements. In Malaysia, the corrosion rate is up to 0.024 mm per year, with estimated costs of $25 billion in 2024 [1]. This ubiquitous degradation is not confined to uniform material loss; it often manifests as localised attacks, as in pitting corrosion. Pitting corrosion initiates localised cavities within the metal surface, fuelled by electrochemical reactions with aggressive anions such as chloride ions (Cl^-). Pitting corrosion severity is based on chloride ion concentration, which can initiate pit growth and merging, undermining the pipeline's structural integrity. Aside from pitting, pipelines are also exposed to other forms of corrosion, such as sweet corrosion (caused by CO_2), sour corrosion (caused by H_2S), and microbiologically influenced corrosion (MIC), each with its own set of challenges and speeding up material degradation in a wide range of operational environments [2]. The intricate chemical compositions of crude oil and natural gas, along with severe operating conditions such as high temperature and pressure, further exacerbate these corrosive processes, rendering pipeline integrity a never-ending struggle [3]. To combat corrosion, strategies such as protective coatings, inhibitors, and cathodic protection are used [2]. Protective coatings act as physical barriers for carbon steel pipelines, shielding them from corrosive environments. However, these coatings are static and prone to damage from impact, chemicals, and ageing, leading to micro-cracks that compromise protection [4]. Such damage often necessitates costly maintenance or early replacement, increasing operational expenditure. Traditional coatings are also challenging to apply in remote areas and can be limited by surface preparation. Despite these methods, maintaining long-term barrier integrity and resisting localised corrosion in harsh marine and oilfield environments remains a challenge.

To overcome these drawbacks, self-healing smart coatings provide a more effective and proactive solution, promising better protection and less frequent maintenance [1]. These smart coatings are formulated to detect and autonomously remove damage from biological systems, thereby prolonging the service life of coated structures [5]. The formulation of these intelligent systems has been greatly enabled by recent advances in nanomaterials and encapsulation techniques, especially during the period 2020-2024, which have enabled precise loading and controlled release of active agents [6]. Previous studies have explored combinations such as Al@MZnGO [7], BLO [8,9], and BTA-HNT [8], reporting improvements in barrier properties; however, these systems often lacked the multi-level defence provided by combining pH-responsive release with autonomous self-healing microcapsules. However, despite significant progress, major challenges remain, including reduced durability under prolonged environmental exposure and insufficient evaluation of long-term performance under aggressive chloride-containing environments. Furthermore, although zinc oxide (ZnO) has been widely reported as a functional nano-additive for corrosion protection, there is still no systematically defined optimal

***CORRESPONDING AUTHOR | F.H.A. Rahim** | ✉ fathin.rahim@utp.edu.my

concentration for dual-layer smart coating systems, particularly when integrated with self-healing microcapsules and nanocarriers. This study designed a dual-layer smart coating system incorporating a hybrid corrosion inhibitor to improve durability for carbon-steel pipeline protection. The top layer is composed of zinc oxide nanoparticles modified with stearic acid (ZnO-STA) as a primary corrosion inhibitor, utilising ZnO's well-known barrier-forming ability and its capacity to release inhibitive ions, while STA enhances hydrophobicity and dispersion [4]. The bottom layer is composed of benzotriazole-loaded halloysite nanotubes (BTA-HNT) and boiled linseed oil microcapsule (BLO-MC) for secondary inhibition. This hybrid system takes advantage of ZnO's barrier-forming ability and the pH-responsive release of BTA from HNTs, which creates a protective film on the metal surface, and the self-healing function of BLO-MC, which releases healing agents in response to damage to seal cracks [5,10,11]. This dual-layer smart coating strategy provides long-lasting protection by complementing immediate surface passivation with slow-release inhibitors, developing a self-adaptive defence against both uniform and localised corrosion under aggressive environments.

The main objective of this study is to investigate the influence of ZnO-STA, BTA-HNT, and BLO-MC as a hybrid corrosion inhibitor in a novel dual-layer smart coating system. Five coating specimens will be developed, including a pure epoxy coating, a traditional dual-layer self-healing coating, and hybrid dual-layer coatings with varying ZnO-to-epoxy ratios (2:1, 4:1, and 6:1) for a comprehensive comparison. By systematically varying the ZnO-to-epoxy ratio, this study seeks to identify an optimal compositional window that balances nanoparticle dispersion, surface morphology, and electrochemical impedance performance, thereby addressing the existing gap regarding ZnO concentration optimisation in multifunctional smart coatings. Characterisation tests will be carried out using Fourier Transform Infrared Spectroscopy (FTIR) and Scanning Electron Microscopy with Energy-Dispersive X-ray Spectroscopy (SEM/EDX) to confirm successful material incorporation and assess structural performance. Corrosion performance will be evaluated carefully using Electrochemical Impedance Spectroscopy (EIS) and scratch tests to assess barrier protection and self-repair functions. Furthermore, the adhesion properties of the dual-layer smart coating will be evaluated using an adhesion strength test to assess its mechanical properties. The outcomes are expected to advance corrosion protection measures, thereby enhancing the durability and service life of oil and gas pipelines and addressing pertinent industry challenges.

2. Materials and Methods

2.1 Materials

Materials for coating additives include benzotriazole (BTA), halloysite nanotubes (HNT), boiled linseed oil, acetone, polyvinyl alcohol (PVA), urea, formaldehyde, resorcinol, ammonium chloride (NH_4Cl), hydrochloric acid (HCl), zinc oxide nanoparticles, and stearic acid, acquired from Avantis Scientific Sdn. Bhd. Composite coatings were synthesized using EPIKOTE 828 epoxy and LSD308 hardener, acquired from ASACHEM Scientific Sdn. Bhd. on a carbon steel substrate (160 mm × 80 mm × 50 mm).

2.2 Preparation of Functional Nanomaterials and Microcapsules

BTA-loaded halloysite nanotubes (BTA-HNT), boiled linseed oil microcapsules (BLO-MC), and stearic acid-modified ZnO nanoparticles (ZnO-STA) were prepared prior to coating fabrication. For the preparation of BTA-HNT, 0.003 kg of dry HNTs were dispersed in 0.0375 L of a saturated BTA solution in acetone (60 mg/mL). The above suspension was mixed using a vacuum pump, followed by three vacuum cycles. The BTA-loaded HNTs were then immersed in a 0.08 M $CuSO_4$ solution under stirring for one minute. The modified nanotubes were centrifuged at 5000 rpm for 300 s, vacuum-dried, and rinsed three times with ultrapure water. The BTA-HNT was subsequently dried in an oven set to 60° for 1 h [12]. Boiled linseed oil microcapsules were synthesised via in situ polymerisation. Briefly, 0.003 kg of urea, 0.0003 kg of resorcinol, and 0.0003 kg of ammonium chloride were dissolved in 1 L of a 1 wt.% polyvinyl alcohol (PVA) aqueous solution. The pH was adjusted to around 3.0 with hydrochloric acid (HCl). BLO was subsequently mixed into the solution, and the mixture was emulsified at 1000 rpm. 0.009 kg of a 37 wt.% formaldehyde solution was added, and the mixture was maintained at 55° with constant stirring for 10 h [13]. The microcapsules obtained were collected through vacuum filtration and rinsed with xylene [14]. Drying of the microcapsules was carried out in a low-pressure oven at 50°C for 6 h [15]. For the preparation of hydrophobic ZnO nanoparticles, 0.0005 kg of ZnO nanoparticles and 2.5% wt./vol. STA was dispersed in 0.01 L of absolute ethanol, and the mixture was agitated at 180 rpm and heated to 55°C for 300 s. The resulting suspension was then subjected to ultrasonication at 500 W and 20 kHz for 300 s. It is recommended that the authors provide adequate information to enable the work to be replicated. Methods that have previously been published should be referenced, and only relevant modifications should be mentioned [16].

2.3 Preparation of Carbon Steel Substrate

The carbon steel samples were soaked in acetone for 0.5 h. The surface was then abraded through sandblasting with a 400-grade sandpaper. The carbon steel was then rinsed with distilled water, degreased with acetone once more, and left to dry at room temperature.

2.4 Preparation of Epoxy and Smart Coatings

Carbon steel substrates were first coated with a reference epoxy system to serve as the control sample. For this purpose, 0.006 kg of epoxy resin and 0.003 kg of hardener were mixed by mechanical stirring for 600 s. The stirred solution was then poured onto the substrate and left to cure for 168 h. The coating's overall thickness was 500 µm. For the conventional dual-layer smart coating, 5.0 wt.% HNT-BTA and 5.0 wt.% BLO-MC was mixed into 0.005 kg of EPIKOTE 828 epoxy resin with 0.00125 kg of LSD308 hardener. The mixture was stirred for 300 s before being applied in two successive

layers, each 250 µm thick, using a paintbrush. The first layer was cured at 25°C for 48 h before the second layer was applied, resulting in a total coating thickness of 500 µm [8,14,17]. For the hybrid dual-layer smart coating, the bottom layer consisted of the self-healing epoxy system containing 5.0 wt.% HNT-BTA and 5.0 wt.% BLO microcapsules into 0.005 kg of EPIKOTE 828 epoxy resin. Next, 0.00125 kg of LSD308 hardener was added to the mixture and stirred for 300 s. To initiate a uniform dispersion, the mixture was stirred continuously for an additional 600 s [14]. The first layer was then applied onto a cleaned and polished carbon steel substrate using a paintbrush, achieving a thickness of 250 µm. This layer was left cured for 48 h at 25°C. For the top layer, as illustrated in Figure 1, the hydrophobic coating was prepared by adding 0.00015 kg of epoxy resin and hardener to the zinc oxide hydrophobic coating suspension and stirring mechanically for 600 s. The resulting coating was then applied to the carbon steel substrate with a thickness of 250 µm. The substrate was left to dry at room temperature for 24 h [16]. Table 1 shows three different samples were prepared with ZnO-to-EP weight ratios of 2:1, 4:1, and 6:1 for comparative analysis.

Table 1. Weight of hydrophobic coating samples

Sample	Ratio of ZnO: EP	Weight (kg)			
		ZnO	STA	EP	Hardener
2:1 ZnO: EP	2:1	0.0009	0.00075	0.00045	0.00045
4:1 ZnO: EP	4:1	0.00018	0.00015	0.00045	0.00045
6:1 ZnO: EP	6:1	0.00027	0.000225	0.00045	0.00045

*1st layer – cure for 48 hours at 48 h at 25°C

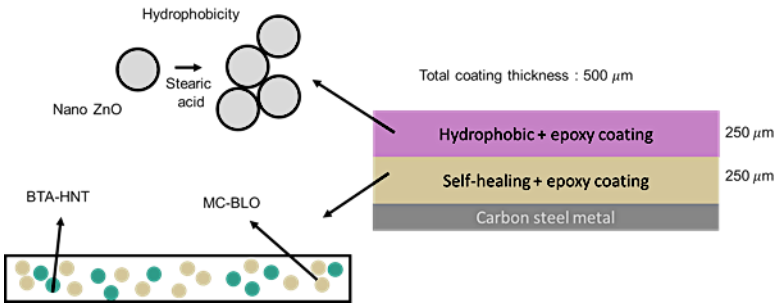

Figure 1. Sketch illustration of ZnO hydrophobic/epoxy and self-healing coating

2.5 Characterization

Fourier Transform Infrared (FTIR) analysis was conducted to confirm the successful integration of BTA-HNT, BLO-MC, and ZnO-STA into the smart coatings. The FTIR spectra were recorded at a resolution of 1 cm^{-1} over the range 400-4000 cm^{-1}. Scanning Electron Microscopy (SEM) combined with Energy-Dispersive X-ray Spectroscopy (EDX) was performed to examine the surface morphology and elemental composition of the coatings, thereby verifying their structural characteristics [16].

2.6 Corrosion and Adhesion Performance Test

Electrochemical Impedance Spectroscopy (EIS) was used to analyse the electrochemical corrosion behaviour of the coating. Following ASTM D1654 for the scratch test and ASTM G31 for the immersion test, the samples were manually scratched over a 50 mm^2 area and submerged in a 3.5 wt.% NaCl solution for 2 weeks. EIS measurements were taken at 0, 7, and 14 days. EIS testing was performed at ambient temperature using a GAMRY 600 System. The setup included an Ag/AgCl reference electrode, a graphite rod counter electrode, and a working electrode prepared according to ASTM G102. Testing was conducted within a frequency range of 0.01 to 100,000 Hz with an AC voltage of 10 mV [1]. Pull-off adhesion testing was performed on five coating samples in accordance with ASTM D4541. The small cylindrical metal dollies and the coated sample surfaces were both cleaned to remove any dust or contamination that might affect the results. Araldite glue was then applied to the doll's surface and attached to the sample surface. Any excess glue around the edges was carefully wiped off to prevent uneven stress distribution during testing. The glue was left to cure for 24 hours. After fully cured, the dolly was removed vertically using the Elcometer 510 automatic pull-off adhesion gauge. The force required to rip the coating away, stated in numerical value (psi), then converted into SI units, MPa, represented the adhesion strength [7]. The adhesion test results for both enhanced hydrophobic and conventional dual-layer smart coatings provide essential data on their long-term corrosion resistance and durability.

3. Results and Discussion

3.1 Fabrication of Coating

All five samples were successfully developed, incorporating three corrosion inhibitors, which are benzotriazole-loaded halloysite nanotubes (BTA-HNT), boiled linseed oil microcapsules (BLO-MC), and zinc oxide with stearic acid (ZnO-STA). Figure 2 illustrates the appearance of carbon steel samples before and after the sandblasting process. Prior to sandblasting, the samples had visible rust and surface contamination, while after sandblasting, the surfaces appeared clean

and free of rust. After the coating process, the thickness measurements for all five samples range from 498 to 501 µm, which conform to the 500 µm specification outlined in the experimental methodology. Figure 3 presents magnified images of each coated sample captured using a tabletop microscope. The EP sample is found to be free of visible contamination, confirming a successful coating process and the absence of foreign substances. In the conventional dual-layer smart coating (DLPC) sample, yellow-colored BLO-MC and green-colored BTA-HNT are visible, indicating successful integration of both corrosion inhibitors. For the hybrid dual-layer smart coating (2:1 ZnO: EP, 4:1 ZnO: EP, and 6:1 ZnO: EP) samples, gaps are observed in the coating. The findings showed that as ZnO concentration increases, gap formation increases as well. Notably, the 6:1 ZnO: EP sample appears more porous compared to the 2:1 and 4:1 ZnO: EP samples. These observations present the critical influence of ZnO concentration on the microstructural characteristics of the developed coatings.

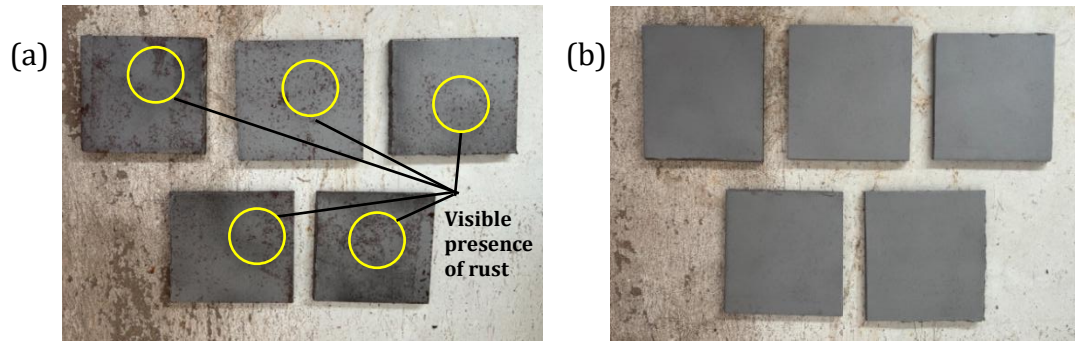

Figure 2. Carbon steel samples (a) before, (b) after the sandblasting process

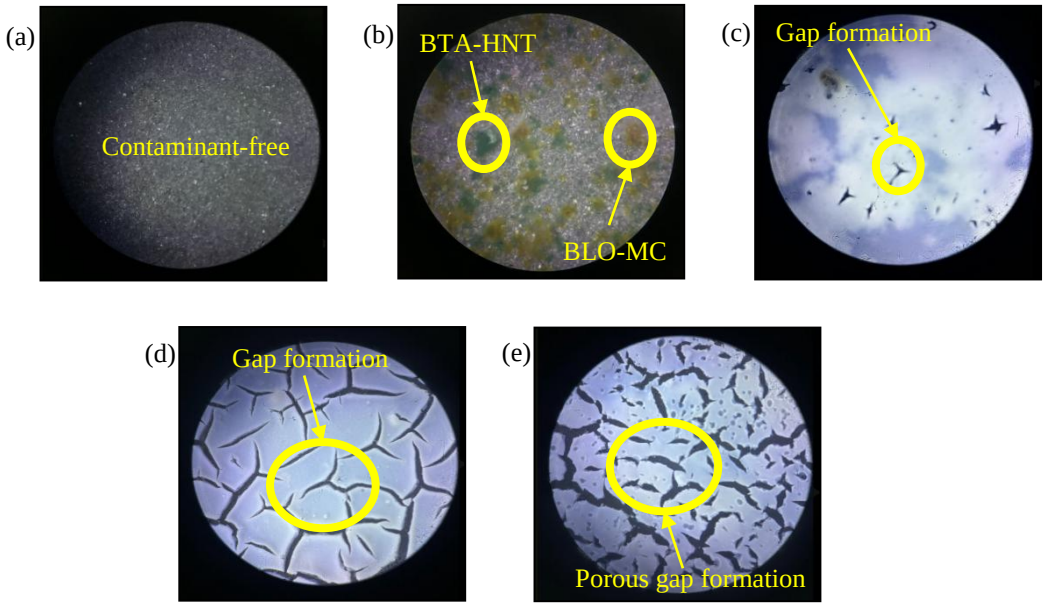

Figure 3**.** Microscopic image of (a) EP sample, (b) DLPC sample, (c) 2:1 ZnO: EP sample, (d) 4:1 ZnO: EP sample, (e) 6:1 ZnO: EP sample

3.2 Characterization

3.2.1 FTIR analysis

FTIR analysis confirmed the successful fabrication of the coating additives BTA-HNT, BLO-MC, and ZnO-STA. The BTA spectrum showed aromatic C-H stretching at 3000–3100 cm^{-1} and C=N stretching at 1450–1500 cm^{-1} [18], while HNT exhibited Si-O-Si stretching at 1000-1086 cm^{-1} and Al-O-Si deformation at 539 cm^{-1} [18,19]. The reduced BTA peaks in BTA-HNT indicated successful encapsulation of BTA within BTA. Both BLO and BLO-MC spectra displayed characteristic C-H stretching at 2850-2971 cm^{-1}, O-H stretching at 3280-3423 cm^{-1}, and C=O stretching at 1746-1751 cm^{-1}, confirming successful microencapsulation of BLO [20, 21]. STA spectrum showed similar C-H stretching at 2850-2971 cm^{-1} and C=O stretching at 1746-1751 cm^{-1}, while ZnO exhibited Zn-O stretching at 450–500 cm^{-1}. RCO_2^- asymmetric stretching at 1540–1580 cm^{-1} at ZnO-STA spectrum confirmed successful formation of zinc stearate [22].

3.2.2 SEM-EDX analysis

SEM-EDX analysis evaluated the samples' distinctive structures, elemental characteristics, and elemental weight percentages in each coating. Figure 4 displays the surface characterisation of all samples. The EP sample shows no signs of contamination, confirming successful fabrication. In the DLPC sample, the presence of both BTA-HNT and BLO-MC indicates the effective integration of self-healing additives. Meanwhile, the 2:1, 4:1, and 6:1 ZnO: EP samples exhibit gap

formation. However, the 6:1 ZnO: EP sample exhibits coating fibre breakage due to excessive ZnO nanoparticle concentration. This leads to the formation of large, irregular structures with a non-uniform distribution and oversaturated zinc stearate crystals, as shown in Figure 5. The elemental composition of each sample, as detailed in Table 2, provides further insight into the coating elemental composition.

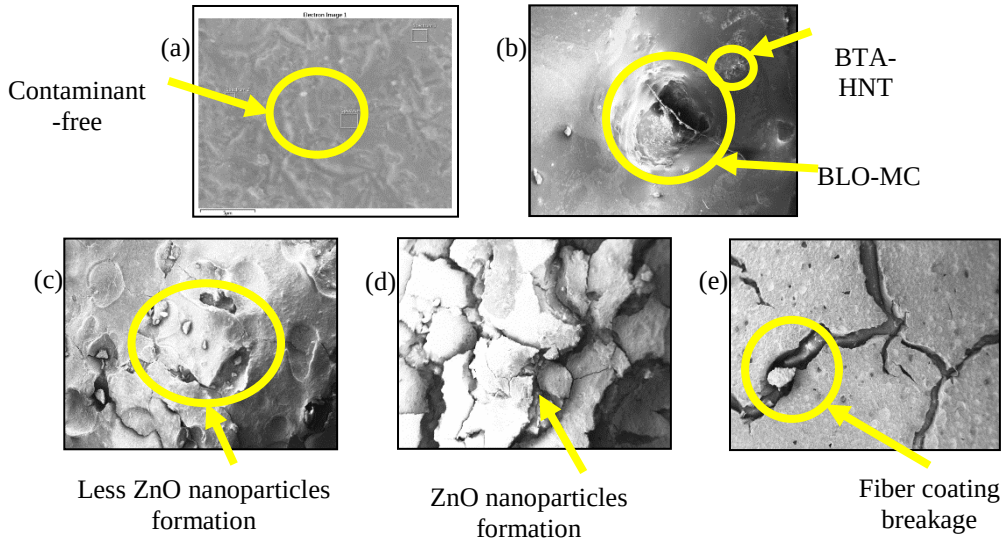

Figure 4. SEM images of (a) EP sample; (b) DLPC sample; (c) 2:1 ZnO:EP sample; (d) 4:1 ZnO:EP sample; (e) 6:1 ZnO:EP sample

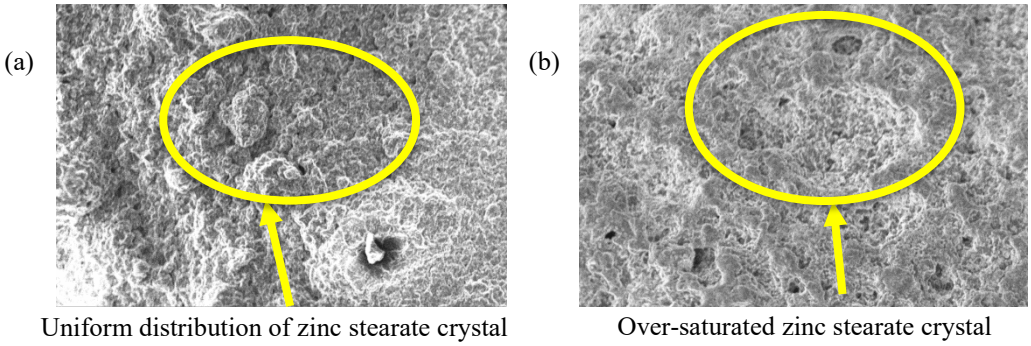

Figure 5. SEM images analysis under 400x magnification of (a) 4:1 ZnO:EP sample; (b) 6:1 ZnO:EP sample

Table 2. Elemental composition of each sample

EP		DLPC		2:1 ZnO: EP		4:1 ZnO: EP		6:1 Zno: EP	
Atom	wt.%	Atom	wt.%	Atom	wt.%	Atom	wt.%	Atom	wt.%
C	90.2	C	68.9	C	69.9	C	47.5	C	29.9
O	9.8	O	25.9	Zn	19.7	Zn	40.4	Zn	56.0
		Al	3.3	O	10.4	O	12.1	O	14.1
		Si	1.1						
		Cu	0.8						

3.3 Corrosion Performance

A corrosion analysis using Electrochemical Impedance Spectroscopy (EIS) with scratch test evaluated the self-repair performance of a hybrid dual-layer coating and a conventional dual-layer coating on carbon steel. The samples were immersed in a 3.5 wt.% NaCl solution for two weeks to assess the coating's impedance performance. Figure 6 (a,c,e) presents Bode plots for various coatings over two weeks. At week 0, the 4:1 ZnO: EP sample showed the highest impedance magnitudes across the frequency range, particularly at lower frequencies. This suggests that the coating has a superior barrier property. Higher impedance (|Z|) indicates greater resistance to charge transfer, indicating the presence of a more protective coating layer that reduces the corrosion rate and enhances corrosion resistance; meanwhile, a higher phase angle (θ) signifies capacitive behaviour, which implements the characteristic of a well-protected surface and slows down the corrosion rate [16]. Meanwhile, pure epoxy shows lower impedance, suggesting a less ideal barrier at the outset. As immersion time increases from week 1 to week 2, a general trend of decreasing impedance magnitude at lower frequencies is observed for all coatings. The gradual degradation of their protective capabilities occurs as the electrolyte

penetrates the coating and reaches the substrate. However, the 4:1 ZnO: EP coating consistently maintains a relatively high impedance magnitude.

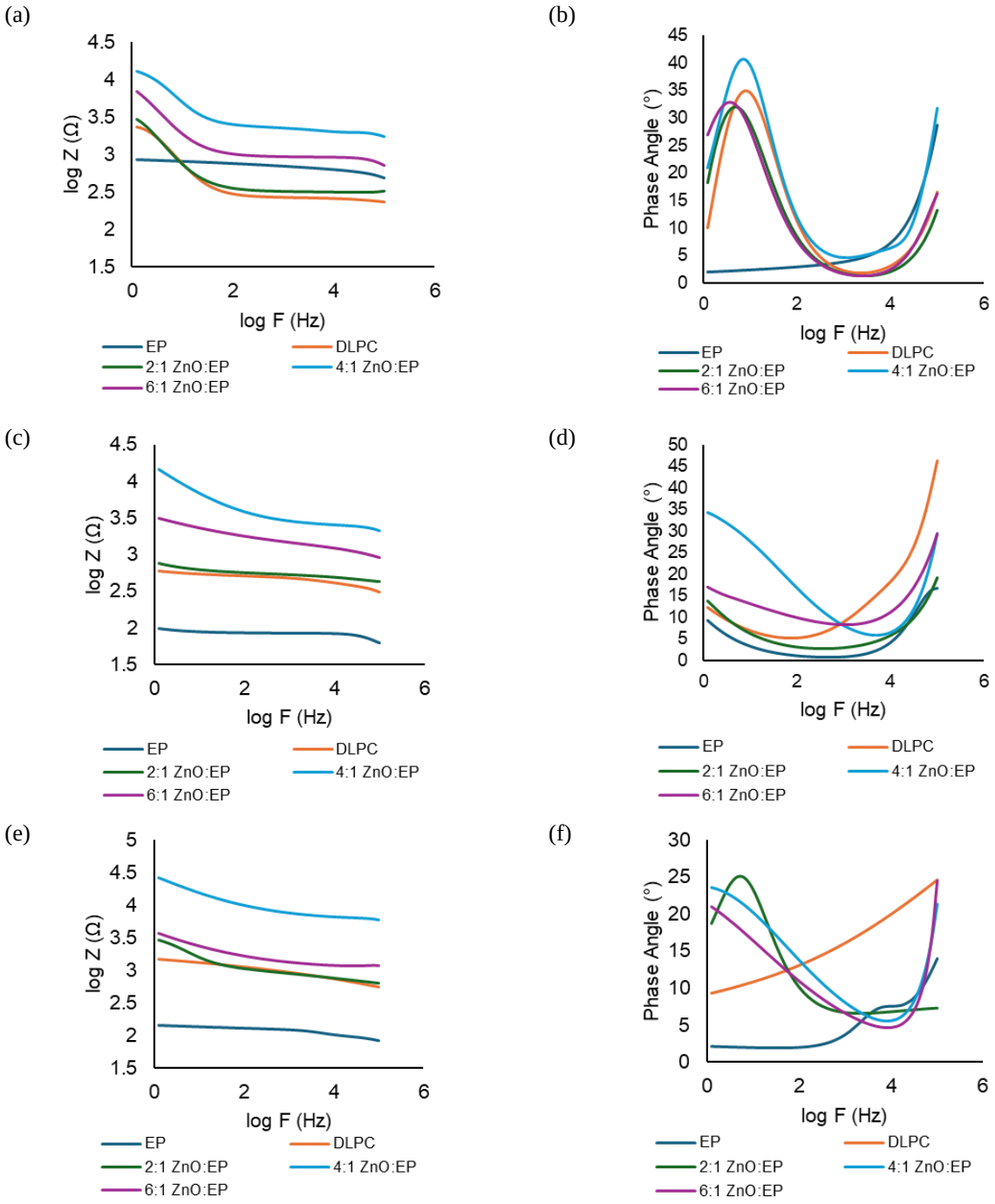

Figure 6. EIS bode magnitude plot and phase angle plot of each sample at (a,b) Week 0; (c,d) Week 1; (e,f) Week 2

In Figure 5(a), impedance at 0.1 Hz of 4:1 ZnO: EP sample ranged from 4.45 Ω to 4.16 Ω, confirming consistent high performance, attributed to ZnO's role in increasing charge transfer resistance and forming a dense, stable layer that blocks water and corrosive agent, mainly in the form of chloride ion from NaCl solution, while lowering interfacial capacitance. This minimizes chemical interactions between the coating and corrosive agents in the salt solution, thereby maintaining the coating's integrity over time by limiting moisture accumulation and salt deposition [23]. Furthermore, the 4:1 ZnO: EP sample exhibited superior corrosion resistance compared to the other formulations. The 2:1 ZnO: EP coating likely contained insufficient ZnO to establish an effective indirect diffusion pathway, thereby limiting its barrier efficiency. In contrast, excessive ZnO loading at 6:1 led to particle agglomeration, resulting in structural inhomogeneity and defect formation within the epoxy matrix, thereby reducing impedance performance.

Surface roughness analysis further supports this observation. The 4:1 ZnO: EP coating exhibited higher roughness values (R_q = 47.53 µm; R_a = 34.72 µm) compared to the 6:1 ZnO: EP coating (R_q = 33.29 µm; R_a = 22.30 µm). The reduction in roughness at 6:1 is attributed to nanoparticle agglomeration, which clusters ZnO particles and reduces surface texture uniformity, as shown in Figure 5(b). Although the surface appears relatively smooth, internal structural defects

facilitate electrolyte penetration and chloride-ion diffusion, ultimately leading to lower impedance values. Therefore, optimal nanoparticle dispersion, rather than surface smoothness alone, governs the corrosion protection performance. Scratch test results showed that the 4:1 ZnO: EP had the lowest corrosion area of 4.4% over 2 weeks, surpassing both the EP and the conventional dual-layer coatings. The anti-corrosion mechanism of the 4:1 ZnO: EP sample is illustrated in Figure 8. The ZnO-STA top layer acts as a first barrier, forming a thin air cushion on the metal surface due to zinc stearate. This layer minimises contact between salt solution and the coating, reducing the penetration of corrosive agents and delaying the onset of corrosion. As a result, this coating provides better corrosion resistance than conventional dual-layer coatings. However, over time, the top layers become saturated with water, activating the self-healing bottom layer, which acts as the second barrier. The bottom layer contains BTA-HNT as a corrosion inhibitor and BLO-MC as a self-healing agent. When the coating is damaged from the scratch test, the microcapsules rupture, releasing both the corrosion inhibitor and self-healing agent. This process forms a protective barrier that prevents further corrosion initiation [7, 23].

The phase angle plots provide crucial information about the capacitive and resistive components within the coating systems (Figure 6(b, d, f)). The pure epoxy exhibits a relatively flat phase angle near 0° at low frequencies, suggesting primarily resistive behaviour. At the same time, DLPC and 3 hybrid coatings exhibit distinct phase-angle peaks, indicative of time constants associated with capacitive and charge-transfer processes. As immersion progresses through Week 1 and Week 2, there is a trend toward decreasing peak heights and frequency shifts in most coatings. This is typically indicative of electrolyte ingress into the coating, which increases porosity and leads to the formation of new time constants associated with electrochemical reactions at the compromised substrate-coating interface [24]. By combining all three corrosion inhibitors, this hybrid dual-layer smart coating significantly extends the material's lifespan compared to a conventional dual-layer smart coating as shown in Figure 7. Hence, the optimal ZnO: EP ratio of 4:1, combined with BTA-HNT and BLO-MC as hybrid inhibitors, provided the best corrosion resistance by minimising moisture uptake and chloride penetration. This sample represents the maximum concentration threshold. Exceeding this concentration results in oversaturation, reducing corrosion protection performance across all samples.

Based on the corrosion performance tests, a comparison can be made between ZnO-based hydrophobic coatings and HNT-based inhibitor coatings. ZnO-based hydrophobic coatings primarily function as a moisture and liquid barrier, limiting saltwater penetration and thus reducing corrosion initiation. In contrast, HNT-based inhibitor coatings provide a self-healing function through the controlled release of corrosion inhibitors when coating damage occurs. When only the HNT-based inhibitor coating is applied, the protective performance relies solely on the self-healing mechanism. However, the dual-layer smart coating, combining a ZnO-based hydrophobic layer and an HNT-based inhibitor layer, provides synergistic protection by integrating both water-barrier and self-healing mechanisms. This combination effectively minimises saltwater interaction and reduces corrosion rates on carbon steel even when the coating is mechanically damaged. Differences in formulation strategies are attributed to variations in elemental composition, as confirmed by FTIR and SEM-EDX analyses. Therefore, the hybrid dual-layer coating demonstrates superior corrosion protection compared to conventional dual-layer coatings due to its multiple complementary protection mechanisms.

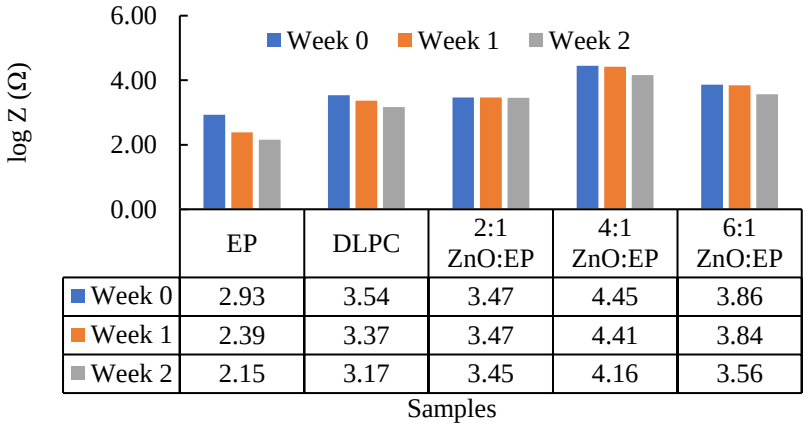

	EP	DLPC	2:1 ZnO:EP	4:1 ZnO:EP	6:1 ZnO:EP
Week 0	2.93	3.54	3.47	4.45	3.86
Week 1	2.39	3.37	3.47	4.41	3.84
Week 2	2.15	3.17	3.45	4.16	3.56

Figure 7. (a) Impedance value of samples at 0.1Hz, (b) Corroded area percentage analysis of samples, for two weeks of immersion

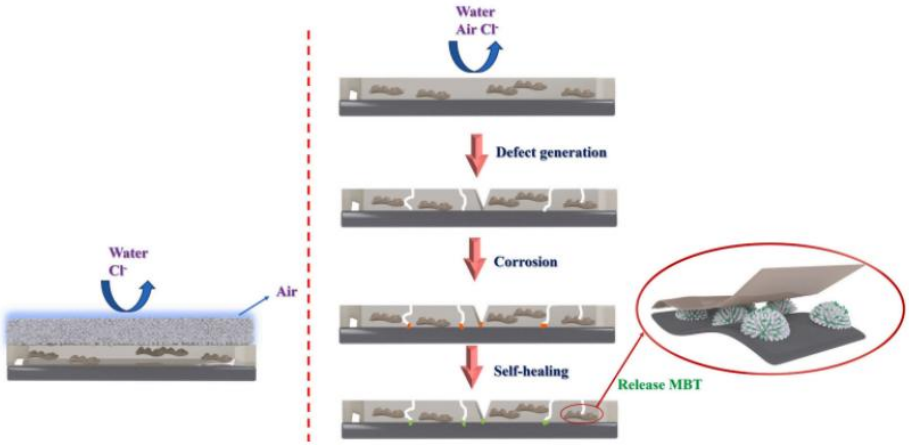

Figure 8. Anti-corrosion mechanism of hybrid dual-layer smart coating composite [1]

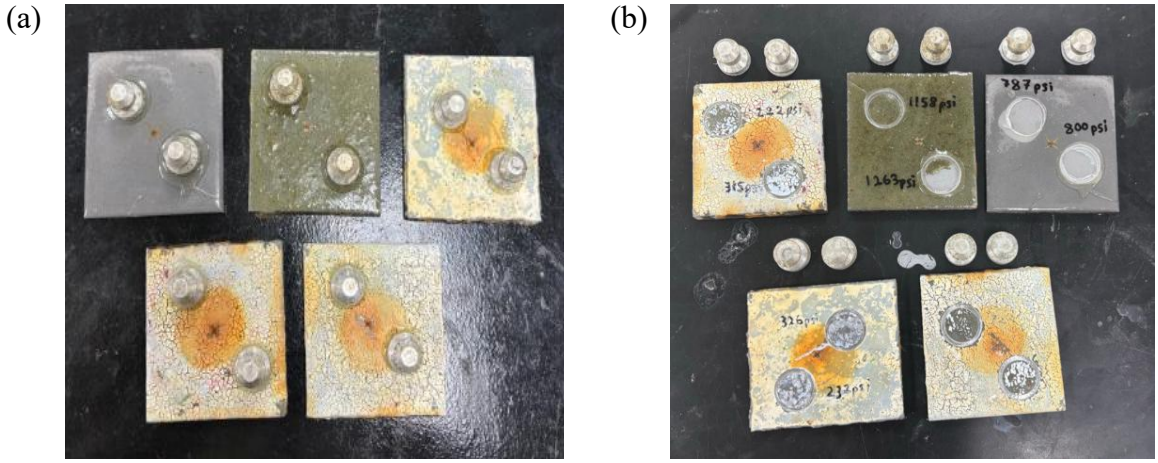

Figure 9. Samples (a) before; (b) after adhesion test

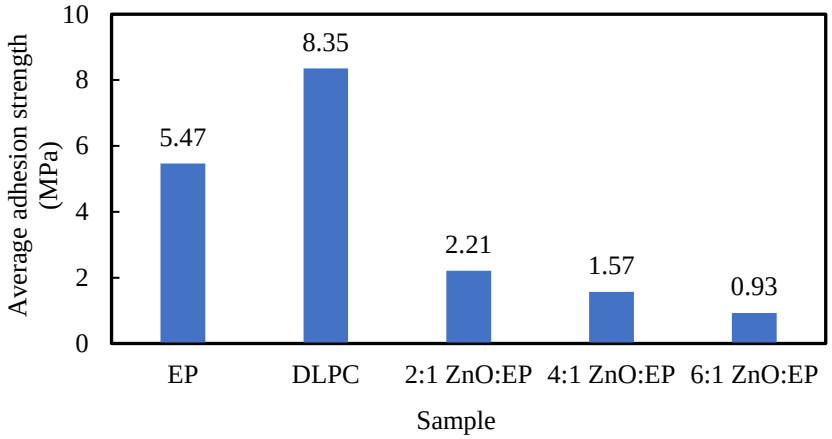

Figure 10. Average adhesion strength of samples after two weeks of immersion

3.4 Adhesion Performance of Coatings

An adhesion test was conducted to evaluate the sample's mechanical bonding under a corrosive environment. Figure 9 shows the experimental process for measuring adhesion strength using the Dolly adhesion test, while Figure 10 presents the average adhesion strength of samples after two weeks of salt immersion. Based on Figure 10, the pure epoxy shows a moderate adhesion strength of approximately 5.5 MPa, serving as the baseline. Due to their lack of active functional groups and insufficient surface interaction, they have limited the overall adhesion [25]. DLPC showed the highest adhesion strength, around 8.2 MPa, and superior performance due to the synergistic effect of the self-healing and corrosion-inhibiting agents. The dual-functional systems can significantly improve the adhesion due to their improved interface compatibility and smart release behaviour under corrosive stimuli. In contrast, the incorporation of a structured nanocomposite layer into the hybrid dual-layer smart coatings (ZnO: EP ratios of 2:1, 4:1, and 6:1) resulted in significantly lower adhesion strength, with a 77.30% reduction compared to the conventional DLPC and EP coatings. This reduction

in adhesion strength is likely due to material incompatibility, which, in turn, weakens the bond between the coating and the metal substrate. The addition of a ZnO-STA coating layer may have introduced a mismatch in the chemical properties of the self-healing BTA-HNT and BLO-MC layers, thereby weakening interfacial bonding. Additionally, overloading can disrupt the epoxy matrix, leading to interfacial stress concentrations and microvoids, as seen in SEM images [26]. Therefore, ensuring material compatibility between both layers is crucial for improving adhesion. Furthermore, the current coating was applied using a brush, which may not be the most effective method in this study. Hence, alternative methods, such as spray coating, should be explored.

4. Conclusions

This study successfully developed both hybrid and conventional dual-layer smart coatings for the corrosion mitigation of carbon-steel pipelines. Three corrosion inhibitors, which are BTA-HNT, BLO-MC, and ZnO-STA, were incorporated and confirmed through FTIR and SEM-EDX analysis, verifying the proper fabrication of the dual-layer smart coatings. EIS and scratch tests confirmed that 4:1 ZnO: EP sample provided the best corrosion resistance with impedance of 4.45 Ω to 4.16 Ω and corrosion area of 4.4% throughout two weeks of experimental observation due to ZnO's ability to form a barrier layer that limits electrolyte penetration while reducing corrosion rate, as well as both BTA-HNT and BLO-MC capability to enhance corrosion inhibition with self-healing mechanism in repairing coating damage. However, adhesion strength was 77.30% lower than that of the conventional dual-layer coating, likely due to incompatibility between the material and the coating application. Overall, the hybrid dual-layer smart coating, integrating ZnO-STA, BTA-HNT, and BLO-MC corrosion inhibitors, demonstrated significant improvement in corrosion resistance compared to the conventional dual-layer smart coating.

Acknowledgements

The authors thank Yayasan Universiti Teknologi PETRONAS for providing the laboratory facilities that enabled this work.

Funding

This work was supported by Yayasan Universiti Teknologi PETRONAS (YUTP) through cost centre 015LC0-519, and by the Centre of Corrosion Research.

Declaration of Competing Interest

The author declares no conflicts of interest.

CRediT Authorship Contribution Statement

K. Jayabalan: Conceptualization, Methodology, Investigation, Data curation, Formal analysis, Writing – original draft.
N.F.C. Lah: Supervision, Conceptualization, Writing – review & editing.
F.H.A.Rahim: Writing – review & editing, Visualization.
P.S. Megat-Yusoff, Abdul Majid, R. Shaharuddin, S., Ramli, S.H.: Visualization, Supervision, Validation, Writing-Reviewing and Editing.

Availability of Data and Materials

Data sharing does not apply to this article as no new data were created or analysed in this study.

Ethics Declarations

This study did not involve human participants or animals. Ethical approval was therefore not required.

Generative Artificial Intelligence Declarations

The authors stated that generative AI was not used to generate content, ideas, or theories. We have just utilised AI to enhance readability and refine the language. This was used with extreme human control and oversight. The authors take full responsibility for reviewing and approving the content.

References

[1] M. A. Azam, S. Sukarti, and M. Zaimi, "Corrosion behavior of API-5L-X42 petroleum/natural gas pipeline steel in South China Sea and Strait of Melaka seawaters," *Engineering Failure Analysis*, vol. 115, p. 104654, 2020.

[2] A. H. Alamri, "Localized corrosion and mitigation approach of steel materials used in oil and gas pipelines – An overview," *Engineering Failure Analysis*, vol. 116, p. 104735, 2020.

[3] U. Sarwar, A. Mokhtar, M. Muhammad, R. K. Wassan, A. A. Soomro, M. A. Wassan et al., "Enhancing pipeline integrity: A comprehensive review of deep learning-enabled finite element analysis for stress corrosion cracking prediction," *Engineering Applications of Computational Fluid Mechanics*, vol. 18, no. 1, p. 2302906, 2024.

[4] Y. Albarqouni, E. Banius, N. H. Abu Bakar, and A. Abdullah, "Enhancing epoxy coatings with spherical ZnO nanoparticles for improved hydrophobicity and corrosion resistance," *Journal of Adhesion Science and Technology*, vol. 39, no. 19, pp. 3009–3029, 2025.

[5] Z. Tian, S. Li, Y. Chen, L. Li, Z. An, Y. Zhang et al., "Self-healing coating with a controllable release of corrosion inhibitors by using multifunctional zinc oxide quantum dots as valves," *ACS Applied Materials and Interfaces*, vol. 14, no. 41, pp. 47188–47197, 2022.

[6] Y. Zhang, M. Yu, C. Chen, S. M. Li, and J. H. Liu, "Self-healing coatings based on stimuli-responsive release of corrosion inhibitors: A review," *Frontiers in Materials*, vol. 8, p. 795397, 2022.

[7] S. Guo, Z. Yu, B. Peng, K. Li, S. Xia, and Y. Chen, "Advanced eco-friendly dual-layer coating: Combining superhydrophobicity with smart self-healing for superior metal protection," *Progress in Organic Coatings*, vol. 197, p. 108774, 2024.

[8] A. Hassanein, A. Khan, E. Fayyad, A. M. Abdullah, R. Kahraman, B. Mansoor et al., "Multilevel self-healing characteristics of smart polymeric composite coatings," *ACS Applied Materials and Interfaces*, vol. 13, pp. 51459–51473, 2021.

[9] M. F. Mamat, M. H. Muhdar, N. N. Dollah, M. R. Kamshah, M. F. Jaafar, L. H. Paijan et al., "Preparation of linseed oil-filled urea-formaldehyde microcapsules and anti-corrosion performance of self-healing epoxy coatings on low carbon steel substrate," *International Journal of Nanoelectronics and Materials*, vol. 17, pp. 61–70, 2024.

[10] D. Xu, C. Lou, J. Huang, X. Lu, Z. Xin, and C. Zhou, "Effect of inhibitor-loaded halloysite nanotubes on active corrosion protection of polybenzoxazine coatings on mild steel," *Progress in Organic Coatings*, vol. 134, pp. 126–133, 2019.

[11] J. Alias, N. A. Johari, A. Zanurin, N. A. Alang, and M. Z. M. Zain, "Self-healing epoxy coating with microencapsulation of linseed oil for the corrosion protection of magnesium (Mg)," *Journal of Physics: Conference Series*, vol. 2129, p. 012008, 2021.

[12] D. Li, B. Gong, Y. Liu, and Z. Dang, "Self-healing coatings based on PropS-SH and pH-responsive HNT-BTA nanoparticles for inhibition of pyrite oxidation to control acid mine drainage," *Chemical Engineering Journal*, vol. 415, p. 128993, 2021.

[13] J. Li, H. Shi, F. Liu, and E. H. Han, "Self-healing epoxy coating based on tung oil-containing microcapsules for corrosion protection," *Progress in Organic Coatings*, vol. 156, p. 106236, 2021.

[14] S. Habib, A. Khan, M. Nawaz, M. H. R. Sliem, R. A. Shakoor, R. Kahraman et al., "Self-healing performance of multifunctional polymeric smart coatings," *Polymers*, vol. 11, no. 9, Art. no. 1519, 2019.

[15] S. M. Mirabedini, M. Esfandeh, R. R. Farnood, and P. Rajabi, "Amino-silane surface modification of urea-formaldehyde microcapsules containing linseed oil for improved epoxy matrix compatibility. Part I: Optimizing silane treatment conditions," *Progress in Organic Coatings*, vol. 136, p. 105242, 2019.

[16] S. W. Yap, N. Johari, S. A. Mazlan, S. N. A. S. Ahmad, R. Arifin, N. A. Hassan et al., "Superhydrophobic zinc oxide/epoxy coating prepared by a one-step approach for corrosion protection of carbon steel," *Journal of Materials Research and Technology*, vol. 25, pp. 5751–5766, 2023.

[17] N. A. Ismail, A. Khan, E. Fayyad, R. Kahraman, A. M. Abdullah, and R. A. Shakoor, "Self-healing performance of smart polymeric coatings modified with tung oil and linalyl acetate," *Polymers*, vol. 13, no. 10, p. 1609, 2021.

[18] Y. Liu, B. Wang, Y. Xie, Y. Chen, Z. Yang, G. Han et al., "A novel dual-responsive halloysite nano-container for anti-corrosion coatings," *Anti-Corrosion Methods and Materials*, vol. 69, pp. 245–252, 2022.

[19] S. Moghari, S. H. Jafari, M. K. Yazdi, M. Jouyandeh, A. Hejna, P. Zarrintaj et al., "In-out surface modification of halloysite nanotubes (HNTs) for excellent cure of epoxy: Chemistry and kinetics modeling," *Nanomaterials*, vol. 11, no. 11, p. 3078, 2021.

[20] M. Mocan and N. B. Sarıkaya, "Sustainable self-healing coatings: Optimizing microencapsulation of biodegradable linseed and hemp seed oils for enhanced corrosion protection," *Journal of Advanced Research in Natural and Applied Sciences*, vol. 10, pp. 845–860, 2024.

[21] K. Thanawala, N. Mutneja, A. S. Khanna, and R. K. Singh Raman, "Development of self-healing coatings based on linseed oil as autonomous repairing agent for corrosion resistance," *Materials*, vol. 7, pp. 7324–7338, 2014.

[22] S. Mostoni, P. Milana, M. D'Arienzo, *et al.*, "Studying stearic acid interaction with ZnO/SiO2 nanoparticles with tailored morphology and surface features: A benchmark for better designing efficient ZnO-based curing activators," *Ceramics International*, vol. 49, pp. 24312–24321, 2022.

[23] J. Sun, J. Wang, W. Xu, and B. Zhang, "A mechanically robust superhydrophobic corrosion-resistant coating with self-healing capability," *Materials & Design*, vol. 240, p. 112881, 2024.

[24] D. Asperti, M. Cabrini, S. Lorenzi, G. Rosace, A. Omrani, and T. Pastore, "Electrochemical impedance spectroscopy analysis of organic epoxy coatings reinforced with nano clay," *Materials*, vol. 17, no. 12, p. 3028, 2024.

[25] Ö. Özkanat, F. M. de Wit, J. H. W. de Wit, H. Terryn, and J. M. C. Mol, "Influence of pretreatments and aging on the adhesion performance of epoxy-coated aluminum," *Surface & Coatings Technology*, vol. 215, pp. 260–265, 2013.

[26] R. Șomoghi, A. Semenescu, V. Pasăre, O. R. Chivu, D. F. Nițoi, D. F. Marcu et al., "The impact of ZnO nanofillers on the mechanical and anti-corrosion performances of epoxy composites," *Polymers*, vol. 16, no. 14, p. 2054, 2024.